



Autosomal recessive *SLC30A9* variants in a proband with a cerebrorenal syndrome and no parental consanguinity

Robert Kleyner,^{1,2} Mohammad Arif,¹ Elaine Marchi,¹ Naomi Horowitz,¹ Andrea Haworth,³ Brian King,³ Maureen Gavin,⁴ Karen Amble,⁴ Milen Velinov,^{1,5} and Gholson J. Lyon^{1,4,6}

¹Department of Human Genetics, NYS Institute for Basic Research in Developmental Disabilities, Staten Island, New York 10314, USA; ²Renaissance School of Medicine (MD Program), State University of New York at Stony Brook, Stony Brook, New York 11794-8434, USA; ³Congenica Limited, BioData Innovation Centre, Wellcome Genome Campus, Cambridge, CB10 1DR, United Kingdom; ⁴George A. Jervis Clinic, NYS Institute for Basic Research in Developmental Disabilities, Staten Island, New York 10314, USA; ⁵Department of Pediatrics, Rutgers Robert Wood Johnson Medical School, New Brunswick, New Jersey 08901, USA; ⁶Biology PhD Program, The Graduate Center, The City University of New York, New York, New York 10010, USA

Abstract An *SLC30A9*-associated cerebrorenal syndrome was first reported in consanguineous Bedouin kindred by Perez et al. in 2017. Although the function of the gene has not yet been fully elucidated, it may be implicated in Wnt signaling and nuclear regulation, as well as in cell and mitochondrial zinc regulation. In this research report, we present a female proband with two distinct, inherited autosomal recessive loss-of-function *SLC30A9* variants from unrelated parents. To our knowledge, this is the first reported case of a possible *SLC30A9*-associated cerebrorenal syndrome in a nonconsanguineous family. Furthermore, a limited statistical analysis was conducted to identify possible allele frequency differences between populations. Our findings provide further support for an *SLC30A9*-associated cerebrorenal syndrome and may help clarify the gene's function through its possible disease association.

Corresponding author:
gholsonjlyon@gmail.com;
Gholson.J.Lyon@opwdd.ny.gov

© 2022 Kleyner et al. This article is distributed under the terms of the Creative Commons Attribution-NonCommercial License, which permits reuse and redistribution, except for commercial purposes, provided that the original author and source are credited.

Ontology terms: intellectual disability; mild

Published by Cold Spring Harbor Laboratory Press

doi:10.1101/mcs.a006137

[Supplemental material is available for this article.]

CLINICAL PRESENTATION

An autosomal recessive cerebrorenal syndrome associated with pathogenic variants in *SLC30A9* was first reported by Perez et al. in a consanguineous Bedouin family in 2017 (Perez et al. 2017). Although the clinical manifestations of the syndrome are variable, all six individuals investigated had decreased renal function, developmental delays, truncal hypotonia, ataxia, spasticity, camptocormia, and hypertonia of limb muscles.

SLC30A9 is a member of the SLC30 family of zinc transporters (ZnT) responsible for maintaining zinc homeostasis by transporting zinc from the cytosol to organelles and the extracellular space to avoid toxicity (Palmiter and Huang 2004). SLC30 ZnTs have been previously implicated in transient neonatal zinc deficiency, diabetes mellitus, hepatic cirrhosis, polycythemia, hypermagnesemia, dystonia, and parkinsonism (Kambe et al. 2014). Some ZnT proteins have also been implicated in pancreatic, breast, and prostate cancers (Bafaro et al. 2017).

In this case study, we describe a female proband with two distinct, inherited loss-of-function variants in *SLC30A9* presenting with clinical findings similar to those described by Perez et al. To our knowledge, this is the first known case of a possible *SLC30A9*-associated cerebrorenal syndrome in a nonconsanguineous family. The variants were identified through next-generation whole-exome sequencing (WES) and were validated using the Sanger sequencing method. This case study may provide further support for an *SLC30A9*-associated cerebrorenal syndrome and, given this possible gene–disease association, may offer more insight in the role of *SLC30A9* in metabolism and human disease.

The proband first presented to our clinic and agency for service evaluation from the Office of People with Developmental Disabilities in New York State at ~1 yr of age, after referral for microcephaly and developmental delay. A comparison of the clinical features found in the proband and Bedouin kindred reported by Perez et al. is included in Table 1. The family signed informed consent to participate in research and to have the results published.

Table 1. Summary of clinical findings found in the proband, as well as those in the Bedouin kindred described by Perez et al. (2017)

Clinical feature	Proband	Bedouin kindred
Cardiovascular		
Heart murmur (HP:0030148)	-	N/A
Craniofacial		
Abnormality of cranial sutures (HP:0011329)	-	N/A
Craniosynostosis (HP:0001363)	-	-
Facial hypotonia (HP:0000297)	+	-
Long eyelashes (HP:0000527)	+	-
Up-slanted palpebral fissure (HP:0000582)	+	-
Developmental		
Failure to thrive in infancy (HP:0001531)	+	-
Feeding difficulties (HP:0011968)	+	N/A
Growth delay (HP:0001510)	+	N/A
Severe global developmental delay (HP:0011344) ^a	+	+
Musculoskeletal		
Appendicular hypotonia (HP:0012389)	-	-
Camptocormia (HP:0100595) ^a	-	+
Limb hypertonia (HP:0002509) ^a	-	+
Muscular hypotonia of the trunk (HP:0008936) ^a	+	+
Neurological		
Abnormal brainstem morphology (HP:0002363)	-	-
Abnormal cerebellum morphology (HP:0001317)	-	-
Abnormal cerebral vascular morphology (HP:0100659)	-	-
Abnormal cerebral ventricle morphology (HP:0002118)	-	-
Abnormal cerebral white matter morphology (HP:0002500)	+	+/-
Abnormal CNS myelination (HP:0011400)	-	+/-
Abnormality of the pituitary gland (HP:0012503)	-	-
Agenesis of corpus callosum (HP:0001274)	+	-
Arachnoid cyst (HP:0100702)	+	-
Bilateral ptosis (HP:0001488)	-	+

(Continued on next page.)

Table 1. (Continued)

Clinical feature	Proband	Bedouin kindred
Dystonia (HP:0001332) ^a	+	+
Limb Ataxia (HP:0002070) ^a	N/A	+
Gray matter heterotopia (HP:0002282)	-	-
Hydrocephalus (HP:0000238)	-	-
Microcephaly (HP:0000252)	+	-
Oculomotor apraxia (HP:0000657) ^a	-	+
Optic atrophy (HP:0000648)	+	N/A
Pachygyria (HP:0001302)	+	-
Progressive sensorineural hearing impairment (HP:0000408)	+	N/A
Strabismus (HP:0000486)	N/A	+
Obstetrical/neonatal		
Abnormality of the abdominal organs (HP:0002012)	-	N/A
Intrauterine growth restriction (HP:0001511)	+	-
Neonatal respiratory distress (HP:0002643)	+	-
Two-vessel umbilical cord (HP:0001195)	+	-
Renal		
Abnormal renal morphology (HP:0012210)	-	+
Renal hypoplasia (HP:0000089)	+	-
Stage 3 chronic kidney disease (HP:0012625)	+	+
Serum		
Abnormal circulating acetylcarnitine concentration (HP:0012071)	+/-	-
Increased circulating creatine kinase MB isoform (HP:0032232)	+	-

(NA) Not available, (-) is not present, (+) is present.

^aFeatures found in all six individuals in the Bedouin kindred.

The proband was born at full term gestation via an uncomplicated vaginal delivery to a mother (age range 20–25) (Fig. 1). There was no notable maternal family history of consanguinity, intellectual/developmental disabilities, or seizures. The father reportedly had a relative with developmental delay. The mother reported having regular prenatal visits and ultrasound examinations, during which a two-vessel umbilical cord was noted. The fetus was reportedly active, and the pregnancy was otherwise unremarkable. The mother denied medication use, preeclampsia, illness, or chemical exposure during pregnancy.

At birth, the proband was jaundiced and small for gestational age, weighing 5 lb (2.3 kg) at birth. She required ventilator support but was discharged 2 d after birth. The mother reported that an abdominal ultrasound was performed on the infant prior to discharge that revealed no abnormalities.

An evaluation by a pediatric neurologist at around age range 0.5–1 yr noted truncal hypotonia, slow weight gain, and severe global developmental delay. The proband smiled, laughed responsively, and cooed, but did not babble. She was able to fixate on and track objects. No developmental regression was noted. The head circumference was below the second percentile for her age (37.5 cm), and the height and weight were below the third percentiles. A neurological exam was otherwise unremarkable, with normal hearing noted. A motor exam revealed a normal appendicular tone, good head control, and no growth arrest.

As per medical records, neuro magnetic resonance imaging (MRIs) at around age range 0.5–2 yr revealed possible microcephaly, bilateral white matter loss in the frontal and parietal lobes, pachygyria, agenesis of the corpus callosum, and an arachnoid cyst. There was no

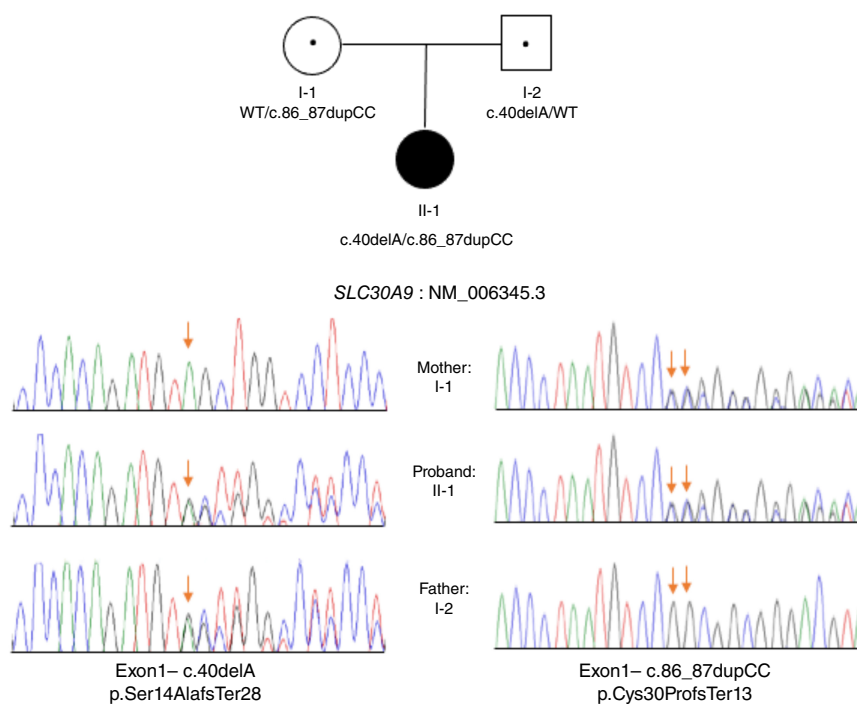


Figure 1. The proband (II-1) carried compound heterozygous frameshift mutations as confirmed by Sanger sequencing: c.40delA inherited from the father (I-2) and c.86_87dupCC from the mother (I-1).

evidence of hydrocephalus, heterotopic gray matter, mass effect, or midline shift. Evaluation of the ventricles, myelination patterns, brain stem, cerebellum, pituitary glands, and vascular flow voids was unremarkable. A skull X-ray conducted several days later revealed patent coronal, sagittal, and lambdoid sutures indicating no evidence of craniosynostosis. Given that the primary data for the MRI and X-rays are not available, imaging is not shown in this report.

This patient first presented to our clinic and agency for services evaluation from the Office of People with Developmental Disabilities in New York State around age range 0.5–2 yr, after referral for microcephaly and developmental delay. The proband was able to sit without support but would bend forward while doing so. While standing, she was unable to bear weight. The proband smiled socially but did not vocalize or laugh. She was receiving speech, physical, and occupational therapy with little improvement. Feeding difficulties were also noted.

Physical examination revealed a height, weight, and head circumference at or below the third percentile (70.5 cm, 7.7 kg, and 40 cm, respectively), which is consistent with previous evaluations. Hypotonia was noted in the trunk and face. Other observed craniofacial abnormalities included arching eyebrows, up-slanting palpebral fissures, and long eyelashes. The parents did not consent for publication of facial photographs. No organomegaly, heart murmurs, nor neurological abnormalities were observed. However, it was noted that the proband did not respond to sound. She was subsequently scheduled for an auditory brain stem response and hearing evaluation that revealed bilateral sensorineural hearing loss.

A follow-up plasma acylcarnitine profile was not specific for a metabolic disorder, but was notable for mildly elevated glutaryl carnitine, malonyl carnitine, decanoyl carnitine, and 3-hydroxy-tetradecenoyl carnitine levels. Further blood work revealed an elevated serum creatine kinase-MB.

Routine blood work at around age range 1–4 yr revealed elevated blood urea nitrogen (BUN) (43 mg/dL) and serum creatinine levels (1.1 mg/dL). The patient was subsequently referred to a pediatric nephrologist. Additional workup confirmed the above laboratory findings and also revealed lymphocytopenia (0.938×10^3 cells/ μ L), elevated cystatin C levels (1.36 mg/L), and elevated parathyroid hormone (PTH) levels (109 pg/mL). The elevated PTH level was suggestive of secondary hyperparathyroidism. The patient had a normal albumin level (4.4 g/dL), phosphorus level (5.4 mg/dL), and platelet count (468,000 thrombocytes/ μ L). The hemoglobin was mildly low (11 g/dL). The proband was prescribed daily calcitriol supplementation, although prior vitamin D levels were within normal limits (32 ng/mL). There was some evidence of mild metabolic acidosis, given a slightly low CO_2 level was measured to be 19 mmol/L, resulting in an anion gap of 16. The glomerular filtration rate (GFR) was considered “poor,” and estimated to be between 25 and 50 mL/min. She was referred for a renal ultrasound examination, which revealed relatively small kidneys (5 cm each), but normal echotexture. Hydronephrosis was not noted. She was subsequently diagnosed with stage 3 chronic kidney disease (CKD). A urinalysis revealed no protein or blood; however, a full report could not be obtained.

The patient’s next follow-up visit was around age range 5–10 yr. She was developmentally delayed, nonambulatory, and nonverbal. Because of food aversion and not eating a sufficient amount of food, she had a gastrostomy tube inserted, although the time of placement was unclear. Physical exam was notable for microcephaly, dysmorphic facial features, and hypotonia. New manifestations included constant facial mimicking and dystonic arm movements. She continued to be followed by a pediatric nephrologist, who reported a “relatively stable” GFR of 40–50 mL/min. She had global developmental delay. It was also documented that she also received cochlear implants several years prior to this and was reportedly able to hear and occasionally respond to commands. At another visit 2 mo later, physical exam revealed no improvement in her microcephaly and motor development and was now notable for constant dystonia affecting the entire body. Blood samples were collected from the mother, father, and the proband for research-based WES, but the family was subsequently lost to follow-up. Laboratory analysis of a blood sample collected several weeks following this visit revealed an elevated BUN (29 mg/dL) and elevated creatinine (0.93 mg/dL), but normal sodium, potassium, chloride, and carbon dioxide levels (138, 4.7, 104, and 19 mmol/L, respectively). The serum calcium level was 9.5 mg/dL, serum phosphorus level was 4.9 mg/dL, and serum albumin was 4.5 g/dL, which are within normal limits. A complete blood count at this time also suggested continuing lymphocytopenia (1.0×10^3 cells/ μ L).

MICROARRAY AND WES ANALYSIS

Cytogenetic analysis of phytohemagglutinin-stimulated cell cultures revealed a normal female karyotype (46,XX) with unremarkable GTG banding patterns. A whole-genome single-nucleotide polymorphism (SNP) chromosomal microarray conducted using the Affymetrix Cytoscan HD platform and the Chromosome Analysis Suite revealed a 505-kb interstitial duplication of 9p24.1-p24.1. This was investigated as a familial variant, but a fluorescence in situ hybridization (FISH) analysis of maternal blood did not suggest that the variant was maternally inherited. Unfortunately, a paternal blood sample was unable to be obtained for FISH analysis. However, analysis of the exome sequencing data showed that this copy-number variant (CNV) is paternally inherited. This duplication includes *KDM4C*, which encodes a lysine demethylase that has been previously implicated in the development and/or progression of certain cancers such as esophageal squamous cell carcinoma (Yang et al. 2000). A recent analysis of a Japanese sample set found significant associations

Table 2. SLC30A9 variants identified in the proband, as well as their protein consequence, predicted effect, parent of origin, and combined annotation-dependent depletion (CADD) score

Gene	Chromosome	Position (hg19)	HGVS DNA reference	HGVS protein reference	Variant type	Predicted effect	dbSNP/dbVar ID	Genotype	ClinVar ID	Parent of origin	CADD score	gnomAD allele frequencies	ACMG evidence strength
SLC30A9	4	41,992,708	NM_006345.3:c.40delA	p.S14AfsX28	Deletion	Frameshift	rs767078182	Heterozygous	VCV001300159	Paternal	23.8	2.17×10^{-5}	PVS1 PM3
SLC30A9	4	41,992,754	NM_006345.3:c.86_87dupCC	p.C30PfsX13	Duplication	Frameshift	rs752245649	Heterozygous	VCV001300169	Maternal	24.6	1.47×10^{-5}	PP4

between CNVs involving *KDM4C* and neuropsychiatric disorders such as schizophrenia and autism spectrum disorder (Kato et al. 2020). However, given the paternal inheritance of this CNV in an unaffected father, it seems likely that this CNV is not contributing to the phenotype described herein.

Samples from the proband (around age range 5–10 yr old) and both parents were sent to Novogene for clinical WES. Variant calling and interpretation were performed using the Congenica platform (Congenica Limited). Coverage and mapping statistics for WES performed on the family are shown in Supplemental Table 1. Two distinct, likely pathogenic, compound heterozygous candidate variants in *SLC30A9* were detected in the proband (NM_006345 c.40delA and c.86_87dupCC), consistent with autosomal recessive inheritance (Table 2). Direct Sanger sequencing supported the presence of both variants in the proband. Sanger sequencing chromatograms are presented in Figure 1. Both variants are predicted to result in nonsense mediated decay and concomitant loss of the encoded protein. Combined Annotation Dependent Depletion (CADD) scores were also calculated for variants (Rentzsch et al. 2019). Both variants had a calculated Phred-scaled CADD score > 20, suggesting that their pathogenicity is predicted to be within the top 1% of all variants.

The following American College of Medical Genetics and Genomics (ACMG) evidence criteria suggesting pathogenicity are as follows: frameshift (i.e., null) variants in a gene in which loss-of-function mutations are a known mechanism of disease (PVS1), detected in *trans* as a pathogenic variant (PM3), and proband's phenotype is highly specific for the gene (PP4). These criteria and other bioinformatic results are also shown in Table 2. Methods are discussed at length in Supplemental Information.

POPULATION ANALYSIS OF SLC30A9 VARIANTS

Given that this proband was of African–American descent, it was hypothesized that variants in *SLC30A9* may be more common in individuals with African ancestry. Pathogenic variants in the gene have also been reported in a Bedouin kindred, who may possess African haplotypes (Abu-Amero et al. 2008). gnomAD was used to identify possible differences in heterozygous missense and loss-of-function (LoF) variant allele frequencies (AFs). AFs were computed for African/African American, Latino/Admixed American, Ashkenazi Jewish, East Asian, Finnish-European, Non-Finnish European, South Asian, and “Other” populations. “Other” populations are represented by individuals who did not cluster with the other populations after a principal component analysis. Given that gnomAD contains 76,156 genomes of individuals with no known medical or family history of severe pediatric disease, it is assumed that the heterozygous variants do not contribute to a cerebrotendinous xanthomatosis if present alone (Karczewski et al. 2020). Summary statistics are included in Supplemental

Table 2 and a PDF of a Python *Jupyter* notebook detailing this analysis is included as Supplemental File 1.

The African/African–American population, as well as the Latino/Admixed American, East Asian, and South Asian populations, had significantly greater missense *SLC30A9* variant AFs when compared to the Ashkenazi Jewish, Finnish–European, and “Other” populations. The calculated missense variant AFs in the non-Finnish European population were significantly greater when compared to the other seven populations analyzed. A heatmap depicting these results is shown in Supplemental Figure 1A. Calculated AFs for heterozygous LoF variants in *SLC30A9* were significantly greater in the African/African–American, East Asian, and South Asian populations than the “Other” and Ashkenazi Jewish populations. Consistent with the findings for missense AFs, the non-Finnish European population had significantly greater AFs than all other populations. These results are displayed as a heatmap in Supplemental Figure 1B.

DISCUSSION

In this report, we present a female proband who is compound heterozygous for two novel LoF variants in *SLC30A9*. There are several similarities between her phenotype and the clinical features reported in a Bedouin family by Perez et al. (2017), such as severe global developmental delay, dystonia, truncal hypotonia, and renal abnormalities. However, the proband did not exhibit camptocormia, limb hypertonia, and oculomotor apraxia, which were consistently present in all six individuals described by Perez et al. The underlying mechanism for the phenotypic incongruity between the described proband and the Bedouin kindred are uncertain but could possibly be attributed to differing fates of transcribed mRNA; the proband’s inherited variants are expected to result in nonsense-mediated decay, whereas the variants observed in the Bedouin kindred are likely translated. Irrespective of these differences, we believe that our findings provide additional support for the existence of a *SLC30A9*-associated cerebrenal syndrome, which in turn emphasizes the gene’s importance in zinc homeostasis.

Individuals with African ancestry do appear to be more likely to carry missense and LoF variants in *SLC30A9* variants when compared to individuals with Ashkenazi Jewish and “Other” gnomAD populations, although individuals with European ancestry appear to be most at risk of carrying these possibly deleterious alleles.

Both experimental and observational studies have demonstrated the role of zinc metabolism in neurological diseases such as neurodegenerative disorders, autism spectrum disorder, movement disorders, amyotrophic lateral sclerosis, mood disorders, traumatic brain injury, strokes, and seizures (Prakash et al. 2015). Zinc released from neuron synapses plays a role in regulating GABA, glycine, *N*-methyl-D-aspartate (NMDA), and α -amino-3-hydroxy-5-methyl-4-isoxazole-propionate (AMPA) receptors (Smart et al. 2004; Szewczyk 2013). Furthermore, zinc has been demonstrated to have a dose-dependent neuroprotective effect, with toxicity noticed at higher dosages (Choi et al. 2020). The *SLC30* family of proteins has specifically been implicated in movement disorders and Alzheimer’s disease (Quadri et al. 2012; Xu et al. 2019). Zinc has also been demonstrated to play a critical role in neural development in utero. Gestational zinc deficiency has been demonstrated to contribute to neural tube defects and other structural abnormalities in rat models, resulting in persistent learning and memory deficits (Brion et al. 2021). These findings are somewhat consistent with observational studies in humans, which suggest a relationship between maternal zinc deficiency and neural tube defects, but no effect of maternal zinc supplementation on cognitive function (Warthon-Medina et al. 2015; Cheng and Gao 2020).

Although the role of zinc transporters and homeostasis in renal pathophysiology is less characterized, several observational studies support the clinical relevance of zinc in renal disease. Individuals with CKD were found to have decreased concentrations of plasma and urinary zinc, as well as an increased fractional excretion of zinc when compared to healthy control subjects (Damianaki et al. 2020). Low serum zinc levels may also be associated with the progression of diabetic nephropathy, given that it was found to be inversely correlated with microalbuminuria and serum creatinine and directly correlated with estimated GFR (eGFR) in diabetic individuals (Al-Timimi et al. 2014). Analysis of data from the Korean Genome and Epidemiology Study suggests a possible causative relationship; individuals whose dietary zinc consumption was calculated to be in the first quartile had a 36% greater risk of developing CKD than those whose zinc intake was in the fourth quartile (Joo et al. 2021).

Experimental studies have mixed results in support of these findings. In rat models, moderate zinc deficiency during the gestational period appears to reduce the activity of renal nitric oxide enzymes and may be associated with reduced renal function in adulthood (Tomat et al. 2007). Furthermore, zinc supplementation has been found to have a protective effect against gentamicin-induced nephropathy in rats (Teslariu et al. 2016). However, in children with CKD, zinc supplementation was found to have a significant positive change in body mass and resulted in “normalization,” but no significant change in serum albumin, zinc, and C-reactive protein (CRP) levels (Escobedo-Monge et al. 2019).

Although the Perez et al. paper reported that the subcellular localization of the protein is unaffected by the mutation, it is important to note that its localization in wild-type cells has not yet been well-characterized. Confocal analysis using SLC30A9 fused to enhanced green fluorescent protein (EGFP) in a neuroblastoma cell line found that the protein is localized in cytosolic vesicles likely associated with the endoplasmic reticulum. However, fluorescence was not observed in the nucleus, which does not align with previous findings, suggesting its role as a nuclear regulator (Perez et al. 2017). It can be speculated that the 63.5-kDa SLC30A9 protein, when fused to the 27-kDa EGFP plasmids, had too low of a nuclear diffusion coefficient to produce a detectable signal (Wei et al. 2003; Dross et al. 2009).

Furthermore, a preprint posted in April 2021 suggests that SLC30A9 acts as a mitochondrial zinc exporter. After exposure to high zinc concentrations, it was reported that the mitochondria in SLC30A9 knockdown HeLa cells had substantially higher zinc concentrations (as measured by the divalent cation-sensitive Rhod-2, AM fluorescent dye) when compared to those in control HeLa cells. The authors also stated that cell toxicity occurs when the SLC30A9 nuclear localization signal is deleted (Kowalczyk et al. 2021). Given that mitochondria have previously been recognized as a possible free zinc storage site, these findings further highlight the importance of SLC30A9 in zinc homeostasis (Lu et al. 2016).

There are several limitations to our conclusions. Although we have made every effort to provide tangible clinical benefit to the proband and her family, clinic visits were sporadic, and the patient was eventually lost to follow-up. Consequently, it is likely that additional clinical features were not presented in this case report, as we were unable to obtain all medical records regarding the proband’s care.

The 9p24.1-p24.1 interstitial duplication (which contains *KDM4C*) was found in the proband, but also was detected in his unaffected father. In addition, the proband’s clinical presentation aligns more with the phenotype seen in the Bedouin family, rather than *KDM4C*-associated disorders such as schizophrenia and autism (Kato et al. 2020). Furthermore, it is also generally accepted that genome duplications tend to be better tolerated than deletions (Brewer et al. 1999).

Our population analysis of SLC30A9 variants in gnomAD also has several limitations. Although the gnomAD database attempts to exclude individuals with severe pediatric disease and their first-degree relatives, it is still possible for some individuals with severe

disease to be included in the data set. Furthermore, given that the allele counts are small, the power of the analysis was limited. It is also important to note that individuals with African ancestry are underrepresented in genomics research and may therefore erroneously appear to have a smaller risk of genetic disease (Bentley et al. 2020).

ADDITIONAL INFORMATION

Database Deposition and Access

The exome sequencing data were generated as part of clinical testing, so the underlying raw data are not consented for deposition to a public database. The variants have been deposited in ClinVar (<https://www.ncbi.nlm.nih.gov/clinvar/>) under accession numbers VCV001300159 and VCV001300169.

Ethics Statement

Both oral and written patient consent were obtained for research and publication, with approval of protocol #7659 for the Jervis Clinic by the New York State Psychiatric Institute—Columbia University Department of Psychiatry Institutional Review Board. Family consent was not given for photography of the children.

Competing Interest Statement

The authors have declared no competing interest.

Referees

Alicia B. Byrne
Anonymous

Received August 2, 2021;
accepted in revised form
October 15, 2021.

Acknowledgments

The authors thank the Genome Aggregation Database (gnomAD) and the groups that provided exome and genome variant data to this resource. A full list of contributing groups can be found at <http://gnomad.broadinstitute.org/about>.

Funding

Funding for this report was provided by the George A. Jervis Clinic of the New York State Institute for Basic Research in Developmental Disabilities (IBR), New York State Office for People with Developmental Disabilities.

REFERENCES

- Abu-Amero KK, Larruga JM, Cabrera VM, González AM. 2008. Mitochondrial DNA structure in the Arabian peninsula. *BMC Evol Biol* **8**: 45. doi:10.1186/1471-2148-8-45
- Al-Timimi DJ, Sulieman DM, Hussen KR. 2014. Zinc status in type 2 diabetic patients: relation to the progression of diabetic nephropathy. *J Clin Diagn Res* **8**: CC04–CC08. doi:10.7860/JCDR/2014/10090.5082
- Bafaro E, Liu Y, Xu Y, Dempski RE. 2017. The emerging role of zinc transporters in cellular homeostasis and cancer. *Signal Transduct Target Ther* **2**: 17029. doi:10.1038/sigtrans.2017.29
- Bentley AR, Callier SL, Rotimi CN. 2020. Evaluating the promise of inclusion of African ancestry populations in genomics. *NPJ Genomic Med* **5**: 5. doi:10.1038/s41525-019-0111-x
- Brewer C, Holloway S, Zawalnyski P, Schinzel A, FitzPatrick D. 1999. A chromosomal duplication map of malformations: regions of suspected haplo- and triplolethality—and tolerance of segmental aneuploidy—in humans. *Am J Hum Genet* **64**: 1702–1708. doi:10.1086/302410
- Brion LP, Heyne R, Lair CS. 2021. Role of zinc in neonatal growth and brain growth: review and scoping review. *Pediatr Res* **89**: 1627–1640. doi:10.1038/s41390-020-01181-z
- Cheng Q, Gao L. 2020. Maternal serum zinc concentration and neural tube defects in offspring: a meta-analysis. *J Matern Fetal Neonatal Med* 1–9. doi:10.1080/14767058.2020.1860930
- Choi S, Hong DK, Choi BY, Suh SW. 2020. Zinc in the brain: friend or foe? *Int J Mol Sci* **21**: 8941. doi:10.3390/ijms21238941

- Damianaki K, Lourenco JM, Braconnier P, Ghobril J-P, Devuyst O, Burnier M, Lenglet S, Augsburger M, Thomas A, Pruijm M. 2020. Renal handling of zinc in chronic kidney disease patients and the role of circulating zinc levels in renal function decline. *Nephrol Dial Transplant* **35**: 1163–1170. doi:10.1093/ndt/gfz065
- Dross N, Spriet C, Zwerger M, Müller G, Waldeck W, Langowski J. 2009. Mapping eGFP oligomer mobility in living cell nuclei. *PLoS ONE* **4**: e5041. doi:10.1371/journal.pone.0005041
- Escobedo-Monge MF, Ayala-Macedo G, Sakihara G, Peralta S, Almaraz-Gómez A, Barrado E, Marugán-Miguelsanz JM. 2019. Effects of zinc supplementation on nutritional status in children with chronic kidney disease: a randomized trial. *Nutrients* **11**: 2671. doi:10.3390/nu11112671
- Joo YS, Kim HW, Lee S, Nam KH, Yun H-R, Jhee JH, Han SH, Yoo T-H, Kang S-W, Park JT. 2021. Dietary zinc intake and incident chronic kidney disease. *Clin Nutr* **40**: 1039–1045. doi:10.1016/j.clnu.2020.07.005
- Kambe T, Hashimoto A, Fujimoto S. 2014. Current understanding of ZIP and ZnT zinc transporters in human health and diseases. *Cell Mol Life Sci* **71**: 3281–3295. doi:10.1007/s00018-014-1617-0
- Karczewski KJ, Francioli LC, Tiao G, Cummings BB, Alföldi J, Wang Q, Collins RL, Laricchia KM, Ganna A, Birnbaum DP, et al. 2020. The mutational constraint spectrum quantified from variation in 141,456 humans. *Nature* **581**: 434–443. doi:10.1038/s41586-020-2308-7
- Kato H, Kushima I, Mori D, Yoshimi A, Aleksic B, Nawa Y, Toyama M, Furuta S, Yu Y, Ishizuka K, et al. 2020. Rare genetic variants in the gene encoding histone lysine demethylase 4C (*KDM4C*) and their contributions to susceptibility to schizophrenia and autism spectrum disorder. *Transl Psychiatry* **10**: 421. doi:10.1038/s41398-020-01107-7
- Kowalczyk A, Gbadamosi O, Kolor K, Sosa J, Andrzejczuk L, Gibson G, St Croix C, Chikina M, Aizenman E, Clark N, et al. 2021. Evolutionary rate covariation identifies SLC30A9 (ZnT9) as a mitochondrial zinc transporter. *Biochem J* **478**: 3205–3220. doi:10.1042/BCJ20210342
- Lu Q, Haragopal H, Slepchenko KG, Stork C, Li YV. 2016. Intracellular zinc distribution in mitochondria, ER and the Golgi apparatus. *Int J Physiol Pathophysiol Pharmacol* **8**: 35–43.
- Perez Y, Shorer Z, Liani-Leibson K, Chabosseau P, Kadir R, Volodarsky M, Halperin D, Barber-Zucker S, Shalev H, Schreiber R, et al. 2017. SLC30A9 mutation affecting intracellular zinc homeostasis causes a novel cerebro-renal syndrome. *Brain* **140**: 928–939. doi:10.1093/brain/awx013
- Prakash A, Bharti K, Majeed ABA. 2015. Zinc: indications in brain disorders. *Fundam Clin Pharmacol* **29**: 131–149. doi:10.1111/fcp.12110
- Quadri M, Federico A, Zhao T, Breedveld GJ, Battisti C, Delnooz C, Severijnen LA, Di Toro Mammarella L, Mignarri A, Monti L, et al. 2012. Mutations in SLC30A10 cause parkinsonism and dystonia with hypermanganesemia, polycythemia, and chronic liver disease. *Am J Hum Genet* **90**: 467–477. doi:10.1016/j.ajhg.2012.01.017
- Smart TG, Hosie AM, Miller PS. 2004. Zn²⁺ ions: modulators of excitatory and inhibitory synaptic activity. *Neuroscientist* **10**: 432–442. doi:10.1177/1073858404263463
- Szewczyk B. 2013. Zinc homeostasis and neurodegenerative disorders. *Front Aging Neurosci* **5**: 33. doi:10.3389/fnagi.2013.00033
- Teslariu O, Pasca AS, Mititelu-Tartau L, Schiriac CE, Gales C, Saftencu PM, Nechifor M. 2016. The protective effects of zinc in experimental gentamicin induced acute renal failure in rats. *J Physiol Pharmacol* **67**: 751–757.
- Tomat AL, Costa MA, Girgulsy LC, Veiras L, Weisstaub AR, Inserra F, Balaszczuk AM, Arranz CT. 2007. Zinc deficiency during growth: influence on renal function and morphology. *Life Sci* **80**: 1292–1302. doi:10.1016/j.lfs.2006.12.035
- Warthon-Medina M, Moran VH, Stammers AL, Dillon S, Qualter P, Nissensohn M, Serra-Majem L, Lowe NM. 2015. Zinc intake, status and indices of cognitive function in adults and children: a systematic review and meta-analysis. *Eur J Clin Nutr* **69**: 649–661. doi:10.1038/ejcn.2015.60
- Wei X, Henke VG, Strübing C, Brown EB, Clapham DE. 2003. Real-time imaging of nuclear permeation by EGFP in single intact cells. *Biophys J* **84**: 1317–1327. doi:10.1016/S0006-3495(03)74947-9
- Xu Y, Xiao G, Liu L, Lang M. 2019. Zinc transporters in Alzheimer's disease. *Mol Brain* **12**: 106. doi:10.1186/s13041-019-0528-2
- Yang ZQ, Imoto I, Fukuda Y, Pimkhaokham A, Shimada Y, Imamura M, Sugano S, Nakamura Y, Inazawa J. 2000. Identification of a novel gene, *GASC1*, within an amplicon at 9p23-24 frequently detected in esophageal cancer cell lines. *Cancer Res* **60**: 4735–4739.